



NLR-TP-98375

Experimental pressure wave research at NLR for high-speed rail tunnels

E.A. Demmenie, A.C. de Bruin, E. Klaver



NLR-TP-98375

Experimental pressure wave research at NLR for high-speed rail tunnels

E.A. Demmenie, A.C. de Bruin, E. Klaver*

* *Project organisation HSL-Zuid*

This paper has been prepared for the EUROMECH Colloquium 379, "Aerodynamics and aeroacoustics of tracked high-speed ground transportation", originally scheduled for September 21 to 23, 1998 at DLR-Göttingen. After the present paper was finished the Colloquium has however been cancelled.

Division:	Fluid Dynamics
Completed:	31 August 1998
Classification of title:	Unclassified



Summary

Pressure waves, that are generated when a high speed train enters a tunnel, can cause annoyance to train passengers (rapid pressure fluctuations acting on the train) and for people living near the tunnel (micro-pressure waves). To improve train passenger comfort the effect of various pressure relieving measures (i.e. shafts and porous walls) were investigated in a sub-scale test. A 1/175 scaled model of a double tracked underwater tunnel, planned for the high speed train link between Amsterdam and Paris, was used. Train models were launched with a facility working according to the air gun principle. Tunnel wall pressure histories generated by the train model were measured. These test results are compared with those predicted by the THERMOTUN/4 calculation method.

With the same air gun facility the steepening of a compression wave in a tunnel and the micro pressure wave emitted from the tunnel exit were studied. The main purpose of this study was to develop the required measurement technique for such tests. The experiments were made in two short tunnel models with an unusually high blockage ratio. These test results are compared with a simple (inviscid) theoretical model and experimental results obtained at SNCF.



Contents

1	Introduction	4
2	Description of the test facility	5
3	Investigation of various pressure-relieving measures in a twin tunnel tube	6
4	The steepening of a compression wave in a tunnel and the micro pressure wave emitted from the tunnel exit	8
5	Concluding remarks	10
	Acknowledgements	11
6	References	12

2 Tabela
11 Figures

(19 pages in total)

1 Introduction

For the integration of the Netherlands in Europe's fast train network a new railway link will be constructed between Paris and Amsterdam. Although the Netherlands are flat country, several double track railway tunnels are planned on this track: two for the passage under rivers ("Dordtse Kil" and "Oude Maas") and one (for environmental reasons) under the so called "green heart" of Holland. The train speeds on this track will be around 300 km/hr.

It is well known (see e.g. Ref. 1) that, when a train enters a railway tunnel with high speeds, strong pressure waves are generated. These propagate down the tunnel and are reflected at the tunnel ends. The resulting rapid changing pressures on a train can cause serious annoyance to the passengers. The strength of the pressure wave is approximately proportional to the square of the train speed and the blockage ratio. Therefore increasing the tunnel cross section can alleviate the problem, but it results in much higher construction costs. The project organisation HSL-Zuid, that designs the track and the tunnels, therefore considered alternative (cheaper) measures such as ventilation shafts and/or a perforated wall between the two tunnel tubes. Their effectiveness was investigated theoretically using the THERMOTUN/4 computer programme developed by A.E. Vardy, reference 2. To verify the theoretical results, it was decided to perform a series of experiments at model scale. To this end, a test facility was built at NLR (see Ref. 3) and several potential pressure reducing measures for one particular tunnel were tested. In the first part of this paper the experimental results will be compared with the theoretical predictions.

The second part of this paper deals with the possible annoyance outside the tunnel, caused by the so-called micro pressure wave. This is due to the fact that when a compression wave hits the tunnel-end, it is reflected back into the tunnel as a rarefaction wave but a small part is transmitted outside the tunnel. To first order (in low frequency approximation), the strength of this micro pressure wave is proportional to the pressure gradient dp/dt of the compression wave at the tunnel exit (Ref. 4). Because a compression wave can steepen up during its passage along the tunnel, it is an issue that can be of special importance for high speed trains in long tunnels.

The steepening of the compression wave and the micro pressure wave were studied in two short (length 0.6 and 1.0 m) tunnels (Ref. 5). The blockage ratio in these tests was quite high (48%). The experiments in the 0.6 m tunnel were similar to those carried out by Grégoire e.a. (Ref. 6), except that at NLR no special gas mixture was needed to attain high Mach numbers. In this paper the experimental results are compared against those of a simple inviscid theoretical model and the results of reference 6.

2 Description of the test facility

Figure 1 depicts the principle of the test facility. It consists of a pneumatic model launcher (“air gun”), an axi-symmetric train model, a tunnel model and data-acquisition equipment. Figure 2 shows a photograph of the train model at the entrance of a test tunnel. A short description of the test facility is given below. For more details on the construction of the facility, see reference 3.

The pneumatic launcher works according to the airgun principle. After rupturing a membrane, the compressed air contained in the “driver” accelerates the train model (with diameter 20 mm) in the launch tube. Normally, the launch tube has a sub-atmospheric pressure and is sealed by a thin membrane that is ruptured by the nose of the train model. The purpose of the dumptank at the end of the launch tube is to collect the air that is pushed forward by the model. It prevents the formation of an air jet and a pressure wave coming out of the launch tube, which could disturb the measurements in the tunnel model. When the model leaves the tube, the back pressure behind the train model is sub-atmospheric and so there is also no blast wave from behind the train model that might disturb the measurements in the tunnel.

After leaving the launch-tube the axi-symmetric model picks up a guidance ring, that slides along two thin piano wires. Before and after the tunnel the train speed is measured using photo electric cells (not shown in Fig. 1).

Pressures inside the tunnel are measured with flush mounted fast responding (Endevco) pressure transducers. The micro-pressure waves are measured with 1/8 inch B&K microphones. These signals are fed to a data-acquisition system (LMS - Leuven Measurements and Systems - with a Scadas Difa front end), where they pass a low-pass filter before being digitalized.

With the test facility train speeds of up to 500 km/hr have been reached. As an illustration figure 3 shows measured pressure traces at mid-tunnel position for a 2.3 m long train in a 7.6 m long tunnel model (blockage ratio 13.5%) for three different train speeds. Note the dramatic increase in pressure wave strength with the increase of train speed.

3 Investigation of various pressure-relieving measures in a twin tunnel tube.

In numerous calculations with THERMOTUN the effect of various pressure-relieving measures for the planned HSL-Zuid twin-tube tunnel under the “Dordtse Kil” river (tunnel length 1330 m) were calculated. From these several typical configurations were selected for testing in the T3F facility. A 1:175 scale tunnel and train model was used for the tests. The 2.3 m long (400 m full-scale) train model had a speed of 300 km/hr. The cross-section of the axi-symmetric train nose was approximately shaped according to that of a TGV train. The location of the shafts and the position of the pressure transducers are shown in figure 4 (all dimensions and times shown are referenced to full scale). The pressure signals were sampled at 20 kHz.

The tunnel configurations tested are summarised in table 1. For tunnel configuration 2 the blockage ratio was 13.5 % (cross-area 70 m²), for all other tests the blockage ratio was 18.9% (cross-area 50 m²). The air shafts (configuration 3 and 5) have a length of about 15 m (full scale) and a cross sectional area of 4.5 m². The perforated separation wall between the two tunnel tubes (configurations 4 and 5) had 0.72m diameter holes. The distance between the holes was 25 m.

Figure 5 shows a comparison of the calculated and the experimental pressure traces at 500 m from the tunnel entrance (the location where the largest changes in tunnel pressure occur) at two blockage ratios and without pressure relieving measures. The agreement between experiment and calculations is very good, though there are some differences in pressure development in the time interval between 2 and 10 seconds (t=0 denotes the entering of the train in the tunnel). These differences are attributed to differences between the simulated (THERMOTUN calculation) and the actual viscous effects in the experiment (e.g. low Reynolds numbers effects). These differences seem to be more pronounced for the low blockage ratio case (Fig. 5b). As shown in reference 3, an almost perfect agreement between calculations and experiment can be obtained when a tapered train model is used to compensate for the Reynolds number effect.

Figure 6a shows that the installation of ventilation shafts is at least as effective as increasing the tunnel cross-sectional area from 50 to 70 m² (compare with Fig. 5b). Also note that the shafts have a pronounced effect on the attenuation of reflected pressure waves from the tunnel ends: pressure fluctuations are low after passage of the train. There is a good agreement between the calculations and experiments even for short duration events (caused by pressure wave reflections at the shafts).

Figure 6b shows that a perforated wall with a relatively small porosity can cause a significant reduction of the strength of the pressure waves (compare Fig. 6b with Fig. 5a). However, the perforated wall has a less direct effect on the attenuation of reflected pressure waves from the tunnel ends than the shafts (compare Figs. 6a and 6b).

Finally, figure 6c shows the results for tunnel configuration 5, which combines the favourable effects of the shafts and the perforated wall.

Similar reductions in pressure wave strength were observed at other positions in the tunnel. A summary of the calculation and test results for maximum pressure change Δp_{\max} at the most critical location (500m from the tunnel entrance) is given in table 1a. In the experiments Δp_{\max} tends to be higher than in the calculations.

So far only the results for pressure wave strength at a fixed position in the tunnel were presented. For the comfort of the train passengers it is more important to investigate the pressure fluctuations on the train. These can directly be obtained from the calculations. In the experiment, pressures on the moving train model were not measured directly. However it can be assumed that the pressure at the tunnel wall equals the pressure at the nearest point on the passing train. By linear interpolation in tunnel wall pressures it is possible to arrive at a (approximated) pressure history for fixed points on the train. It has however to be noted that, due to the limited number of pressure transducers in the tunnel, this procedure leads to an under prediction of maximum pressure changes on the train. A comparison of calculated and experimental (interpolated) maximum pressure changes (and the location where it occurs on the train) is given in table 1b. The percent reductions in maximum pressure change observed on the train appear to be even larger than the maximum pressure changes observed in the tunnel. With combined shafts and a perforated wall the maximum pressure change on the train reduces to about 42%. It is remarked that for the present test conditions the shafts and/or perforated walls are more effective in reducing the maximum pressure fluctuation on the train than increasing the tunnel cross section from 50 to 70 m².

Some remarks should be made here on the application of a perforated tunnel wall between two tunnel tubes. With a perforated tunnel wall, pressure waves and draught velocities develop in the adjacent tunnel tube (see Fig. 7a). In some cases people may be working in the other tunnel tube and in order to keep annoyance levels (pressure and draught) in the adjacent tunnel tube sufficiently low, the perforations in the tunnel wall should not be too large. However, the pressure waves in the adjacent tunnel tube are reduced considerably with ventilation shafts in both tunnel tubes (see Fig. 7b).

4 The steepening of a compression wave in a tunnel and the micro pressure wave emitted from the tunnel exit

To demonstrate the ability to measure the steepening of pressure waves and the subsequent micro pressure wave emitted from a tunnel exit some exploratory tests were made.

A schematic drawing of the test set-up is given in figure 8. In these tests no model guidance ring was used, since this could give a distortion of the compression wave. The tests were performed with two tunnel model lengths (0.6 and 1 m) both having a blockage ratio of 48 % (much higher than in realistic situations). The train speed was 330 km/hr and the resulting compression wave had a strength of about 10 kPa. The dimensioning of the train model nose (hemi-spherical), the flange plates and the positioning of the pressure sensors in the short tunnel resemble precisely the test conditions of reference 6, albeit on a 2.5 times smaller scale. The experiments of reference 6 had to be carried out in a special gas mixture in order to reach the desired Mach number. The present experiments could be carried out in plain air (at much higher train speeds). This, and the smaller model scale, put higher demands on the data-acquisition.

The resonance frequency of the Endevco pressure transducers used for the tunnel wall pressures was larger than 155 kHz. The micro pressure waves were measured with two B&K 1/4 inch microphones (resonance frequency about 90 kHz) with the grid removed and the diaphragm placed perpendicular to the propagation direction of the micro pressure wave (assumed spherical from tunnel exit centre). All the pressure signals passed through a low pass filter (-3 dB point at 80 kHz) before being sampled at 200 kHz by a 12 bits ADC (analogue to digital converter). The discretisation error was 25 Pa.

Figure 9a shows the dimensionless tunnel wall pressure histories (with pressure transducers placed at opposite sides, see Fig. 8) at 80 mm and at 487 mm from the tunnel entrance. The pressure was made dimensionless by dividing with $1/2 \rho V_{tr}^2$ (air density ρ , train speed V_{tr}). During passage of the train nose along the pressure transducers at $x=80$ mm (at $t \approx .0008$ sec) the dimensionless pressure traces differ considerably. This is probably caused by a non axi-symmetric passage of the train model. At 487 mm from the entrance, the pressure wave has steepened up considerably, see figure 9a. The difference between the two pressure traces recorded at this location remains to be further investigated.

The pressure gradient dp/dt was determined from the measured pressure histories by using a time interval of 0.01 msec. It was subsequently made dimensionless by dividing with $1/2 \rho V_{tr}^3 D_{tun}^{-1}$ (D_{tun} = tunnel diameter). Figure 9b shows local dimensionless maximum pressure gradients $K_{gr,max}$ as function of time. Figure 9c shows the corresponding micro-pressure waves recorded at 92 and



184 mm from the tunnel exit of this 1m long tunnel. At double distance the maximum amplitude of the micro pressure wave is about halved (which is to be expected for a spherical expansion of the wave front).

In table 2 some measurement results are presented together with results from reference 6. The train Mach number in all these cases was 0.27. The $C_{p,max}$ value of the Ref. 6 test appears slightly higher than those of the NLR tests. The $C_{p,max}$ values of the NLR tests repeat well. However, large variations in the dimensionless pressure gradient $K_{gr,max}$ are found which may have been caused by a non axial symmetric entering of the train in the tunnel. But this hypothesis needs further investigation.

Differences in initial $K_{gr,max}$ values lead to increased differences further down the tunnel. Measurements that have the same $K_{gr,max}$ at the initial position $x=80$ mm also seem to agree fairly well at $x=487$ mm (e.g. compare 5_1, 6_10 and Ref. 6 result). The amplitude of the micro-pressure wave is related to $K_{gr,max}$, but this relation appears to be less than linear (as predicted by simple theory, Ref. 4). Consequently, the large variation in $K_{gr,max}$ values observed at $x=487$ mm is much less reflected in the amplitude of the micro pressure waves (last column in Tab. 2). It should be noted that due to the continued steepening of the pressure wave in the tunnel, the $K_{gr,max}$ value at the end of the tunnel will probably have been much larger than its value at $x=487$ mm (especially for the 1m long tunnel). For the same reason, the amplitude of the micro pressure wave is somewhat larger for the “long” 1m tunnel than for the “short” 0.6 m tunnel.

For a better understanding of the steepening of the pressure waves in the experiment, supporting calculations were made with a simple inviscid method. The propagation of a compression wave in an inviscid medium is approximately described by the following equation (see e.g. Ref. 4):

$$\frac{\partial u}{\partial t} + \left(c_o + \frac{\gamma + 1}{2} u \right) \frac{\partial u}{\partial x} = 0$$

In this equation u is the velocity disturbance accompanying the passage of the compression wave and ρ_o and c_o are the ambient air density and speed of sound. Note that u is approximately equal to $p/\rho_o c_o$ (where p is the pressure rise with respect to ambient conditions). The equation was solved numerically using a Mac-Cormack (predictor-corrector) method. The initial condition $u(x)$ at $t=0$ was obtained (by suitable approximations) from the recorded pressure history at 80 mm from the entrance. The theoretical calculations slightly over-predict the steepening of the pressure wave (see Fig. 9b), because no tunnel wall friction was assumed. Figure 10 gives a direct comparison of the experimental and calculated $K_{gr,max}$ values along the tunnel for the 6_10 and 6_3 test cases that have different initial conditions (both in shape and $K_{gr,max}$, see Fig. 11). It should be noted that not only the initial $K_{gr,max}$ value but also the shape of the pressure wave has influence on the downstream steepening of the pressure wave, as calculations not presented here demonstrate.



5 Concluding remarks

In the Train Tunnel Test Facility (T3F), constructed at NLR, train model speeds up to 500 km/hr can be attained. For planned Dutch high speed rail tunnels various pressure relieving measures were investigated at a train speed of 300 km/hr using a 1:175 scaled model. It was shown that ventilation shafts and perforated walls can provide a very effective reduction in the strength of the pressure waves. The experimental results agreed well with the theoretical calculations.

With the same facility the steepening of pressure waves and the resulting magnitude of the micro-pressure wave emitted from the tunnel exit were investigated. For these tests a tunnel model with an unusually high blockage ratio was used. This resulted in strong pressure waves which, as in reference 6, showed a substantial steepening during their passage through the tunnel. According to simplified theory (Ref. 4) the micro-pressure wave amplitude should be proportional to dp/dt -max of the incident pressure wave at the tunnel exit. Though the dp/dt max value of the incident pressure wave at the tunnel exit was not measured (it was only measured at $x=487$ mm), the present experimental results seem to indicate a much weaker (less than linear) relationship between dp/dt -max and the amplitude of the micro-pressure wave.

It was observed that, for nominally identical test conditions, substantially different initial pressure waves were created. This is possibly due to a non axi-symmetric entering of the train in the tunnel, which may have been typical for the present tests at high blockage ratio.

Further experiments in tunnels with realistic blockage ratios (and less strong pressure waves) are needed to clarify the steepening of compression waves and the possible influence of viscous effects.



Acknowledgements

The authors want to express their gratitude to the project organisation HSL-Zuid for giving permission to present test results and to Mr. Grégoire of SNCF for providing details of his experimental test set-up.

6 References

1. Gawthorpe, R.G. and Pope, C.W.: *The Measurement and Interpretation of Transient Pressures Generated by Trains in Tunnels*, Proceedings of the 2nd International Symposium on Aerodynamics and Ventilation of Vehicle Tunnels, Cambridge 1976, part C3, pp. 35-55.
2. Vardy, A.E.: *Aerodynamic Drag on Trains in Tunnels, Part 2: Prediction and Validation*, Proceedings Institute of Mechanical Engineers Vol. 210, Part F: Journal of Rail and Rapid Transit, 1996, pp. 39-49.
3. de Wolf, W.B.; Demmenie, E.A.F.A.: *A new test facility for the study of interacting pressure waves and their reduction in tunnels for high-speed trains*, 9th International Conference on Aerodynamics and Ventilation of Vehicle Tunnels, Aosta Valley, Italy, 6-8 October 1997, pp. 301-317.
4. Ozawa, S.; Murata, K.; Maeda, T.: *Effect of ballasted track on distortion of pressure wave in tunnel and emission of micro-pressure wave*, 9th International Conference on Aerodynamics and Ventilation of Vehicle Tunnels, Aosta Valley, Italy, 6-8 October 1997, pp. 935-947.
5. E.A. Demmenie, *Measurement of micro pressure waves near the exit of a high speed rail tunnel model*, NLR Technical Report (to be published).
6. Grégoire, R.; Réty, J.M.; Masbernat F.; Morinière, V.; Bellenoue, M.; Kageyama T.: *Experimental study (scale 1/70th) and numerical simulations of the generation of pressure waves and micro-pressure waves due to high-speed railway-tunnel entry*, 9th International Conference on Aerodynamics and Ventilation of Vehicle Tunnels, Aosta Valley, Italy, 6-8 October 1997, pp. 877-903.

Table 1a Maximum pressure change in the tunnel (at 500 m (full scale) from tunnel entrance)

Configuration		THERMOTUN	Measurement
		Δp_{\max} [kPa]	Δp_{\max} [kPa]
1	blockage ratio 18.9 %	8.2	8.55
2	blockage ratio 13.5 %	5.6	6.4
3	Ventilation shafts, blockage ratio 18.9 %	5.6	6.0
4	Perforated wall, blockage ratio 18.9 %	5.8	6.4
5	shafts + perfor. walls, blockage ratio 18.9%	4.6	5.15

Table 1b Maximum pressure change on the train

Configuration	THERMOTUN/4		Measurements NLR	
	Δp_{\max} [kPa]	Position	Δp_{\max} [kPa]	Position [% train length]
1	5.5	nose	5.3	5
2	3.8	nose	3.9	5
3	2.9	1/3 train	2.9	25
4	3.2	tail	3.05	70
5	2.3	tail	2.15	70

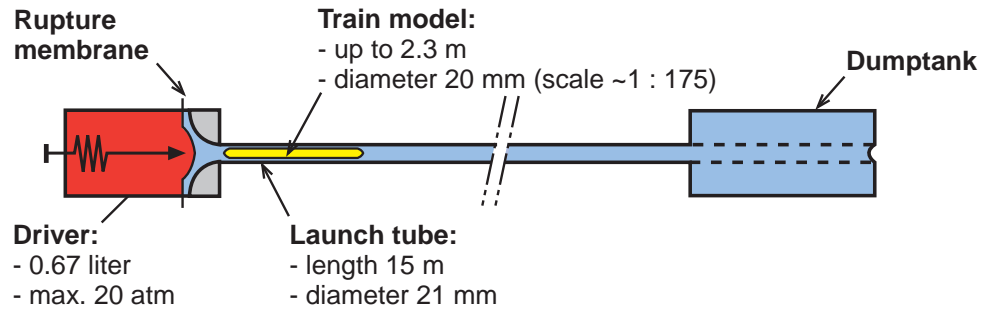
Table 2 $C_{p,\max}$, $K_{gr,\max}$ and micro pressure wave strength at 92 mm from the tunnel exit

Case	Tunnel Length [m]	Train Speed [m/s]	$C_{p,\max}$ x= 80 mm	$C_{p,\max}$ x= 487 mm	$K_{gr,\max}$ x= 80 mm	$K_{gr,\max}$ x= 487 mm	B&K [Pa]
5_1	0.6	92.7	1.7	1.6	3.3	5.9	420
5_9	0.6	90.8	1.8	1.6	4.5	8.9	480
5_11	0.6	91.5	1.7	1.6	2.8	4.2	350
6_3	1.0	91.2	1.8	1.7	4.5	9.4	555
6_10	1.0	91.0	1.7	1.7	3.4	6.0	520
Ref. 6*			1.9	1.75	3.5	5.7	350

*) **Note:** These measurements were carried out using a heavy gas mixture enabling to attain the same Mach number at a lower train speed (50 m/s). The tunnel length corresponds with the 0.6m long tunnel.



Air gun



Test tunnel

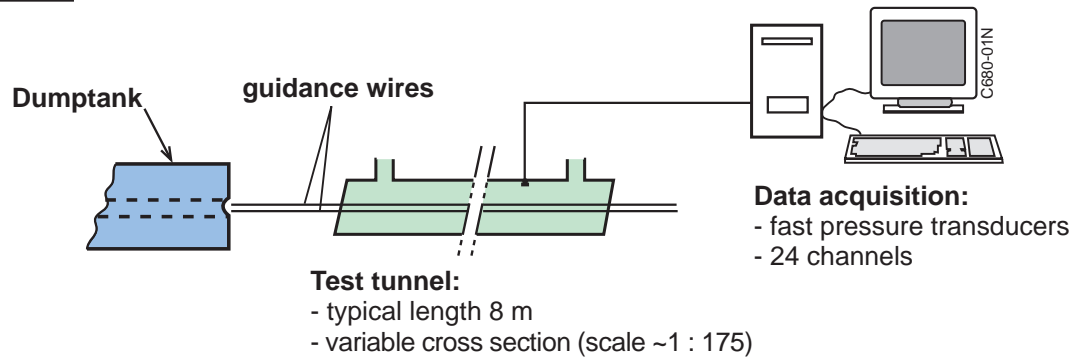


Fig. 1 Principle of the facility



Fig. 2 Train model entering the tunnel

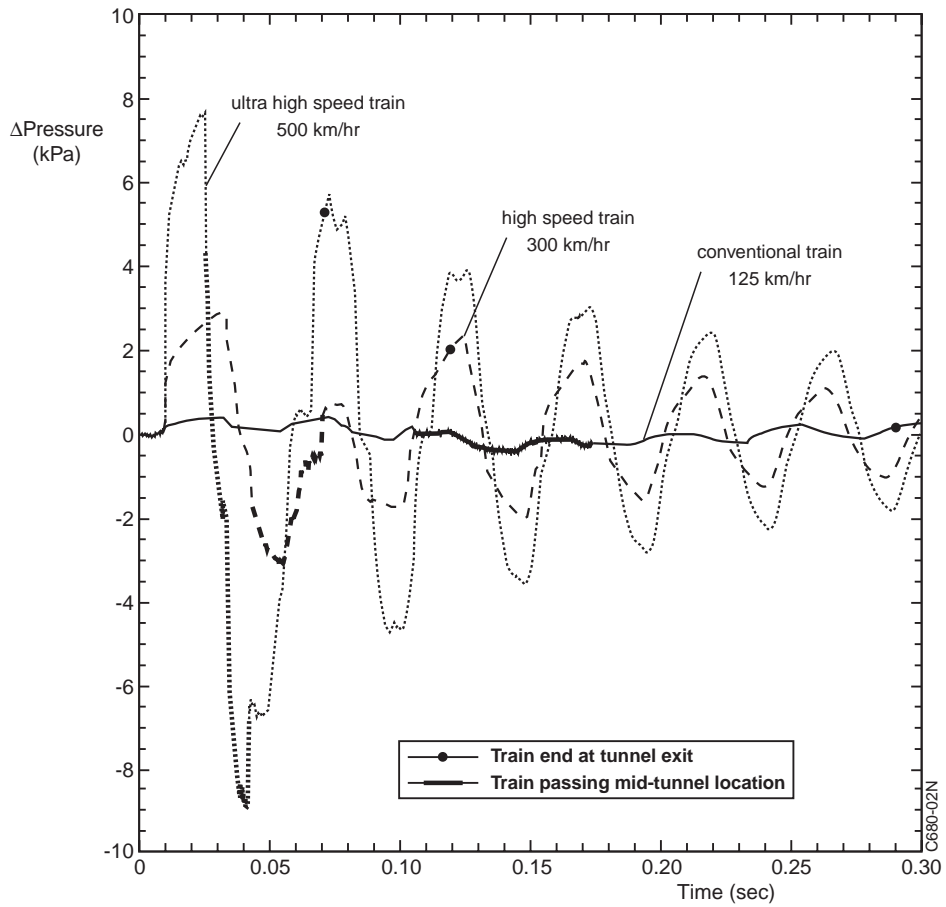


Fig. 3 Measured pressure histories at mid-tunnel position for three train velocities

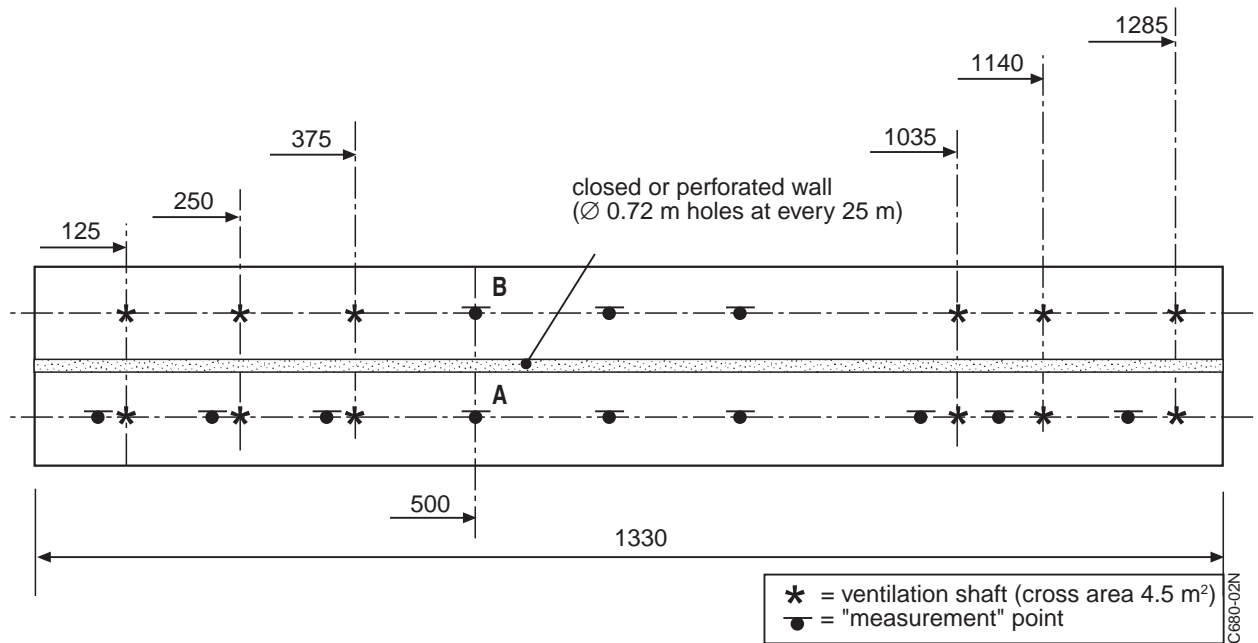


Fig. 4 Location of ventilation shafts and pressure transducers in the tunnel model (Note: the dimensions are translated to the full scale situation)

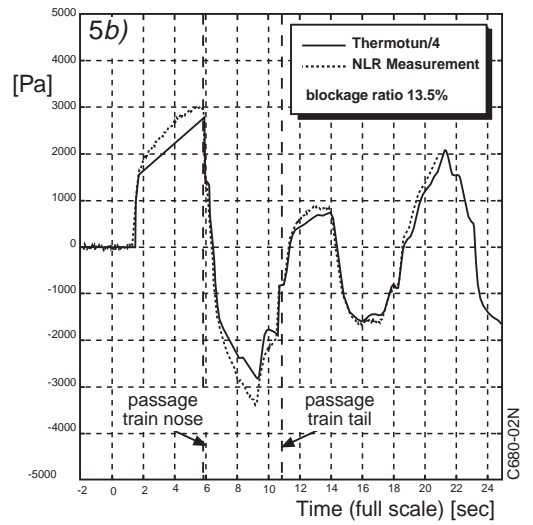
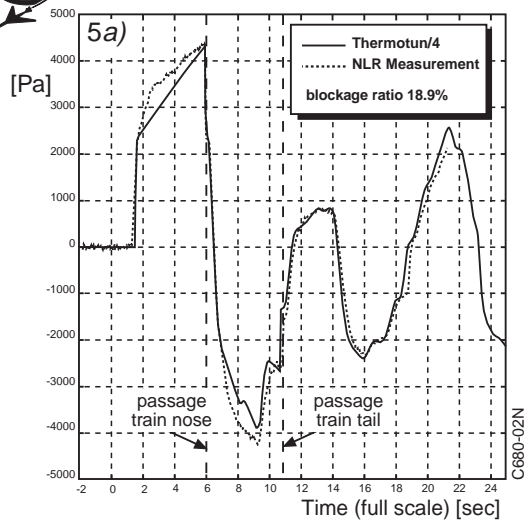


Fig. 5 Effect of blockage ratio on tunnel wall pressure history (train speed 300 km/hr; location A, see Fig. 4)

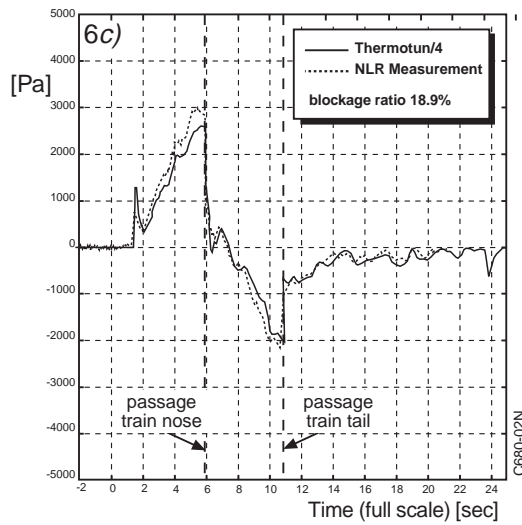
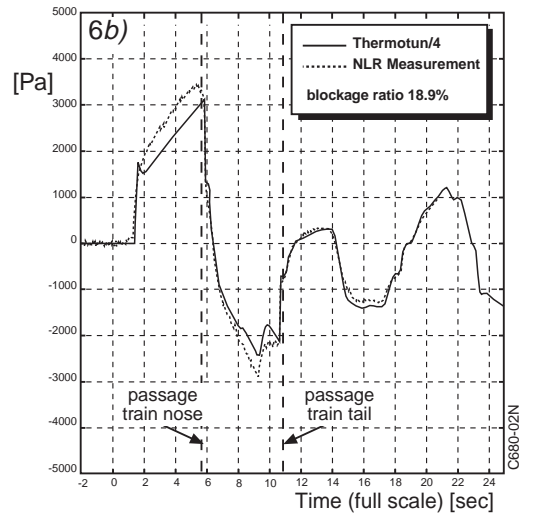
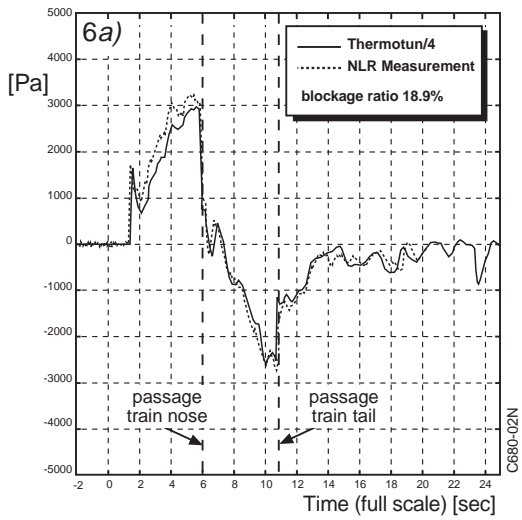


Fig. 6 Reduction of tunnel wall pressures by application of: a) shafts, b) a porous wall and c) a combination of both (train speed 300 km/hr; location A, see Fig. 4)

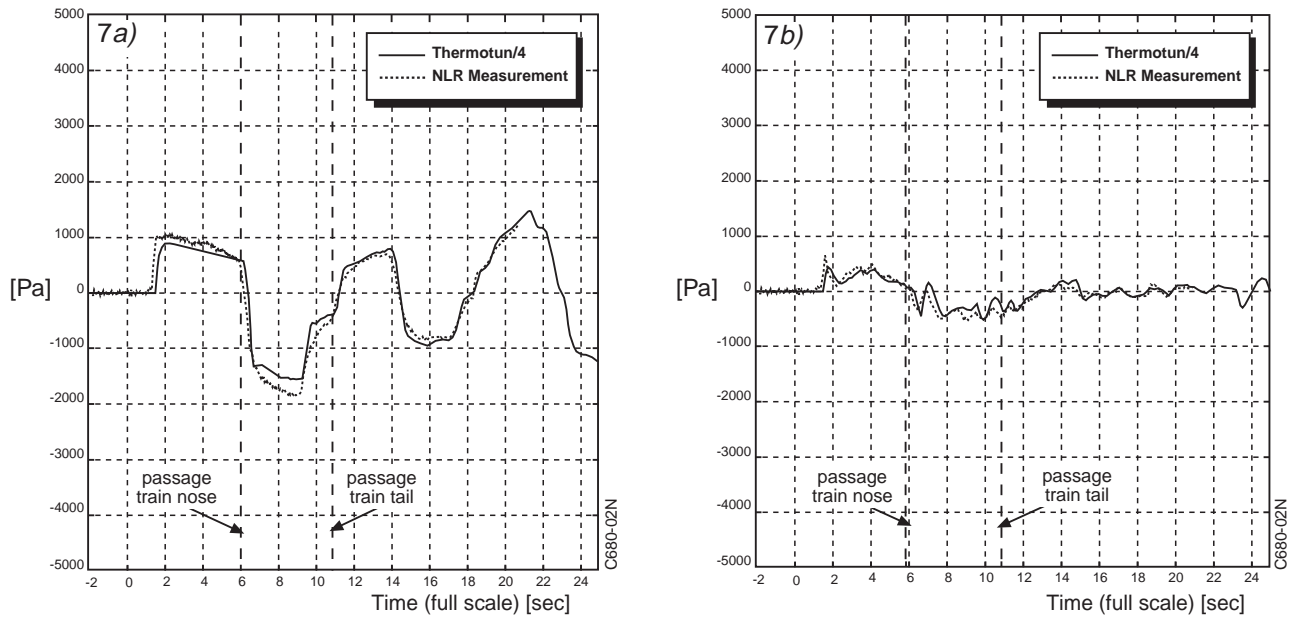


Fig. 7 Effect of a perforated separation wall on the pressure history in the adjacent tunnel tube: a) without shafts, b) with shafts (train speed 300 km/hr; location B, see Fig. 4)

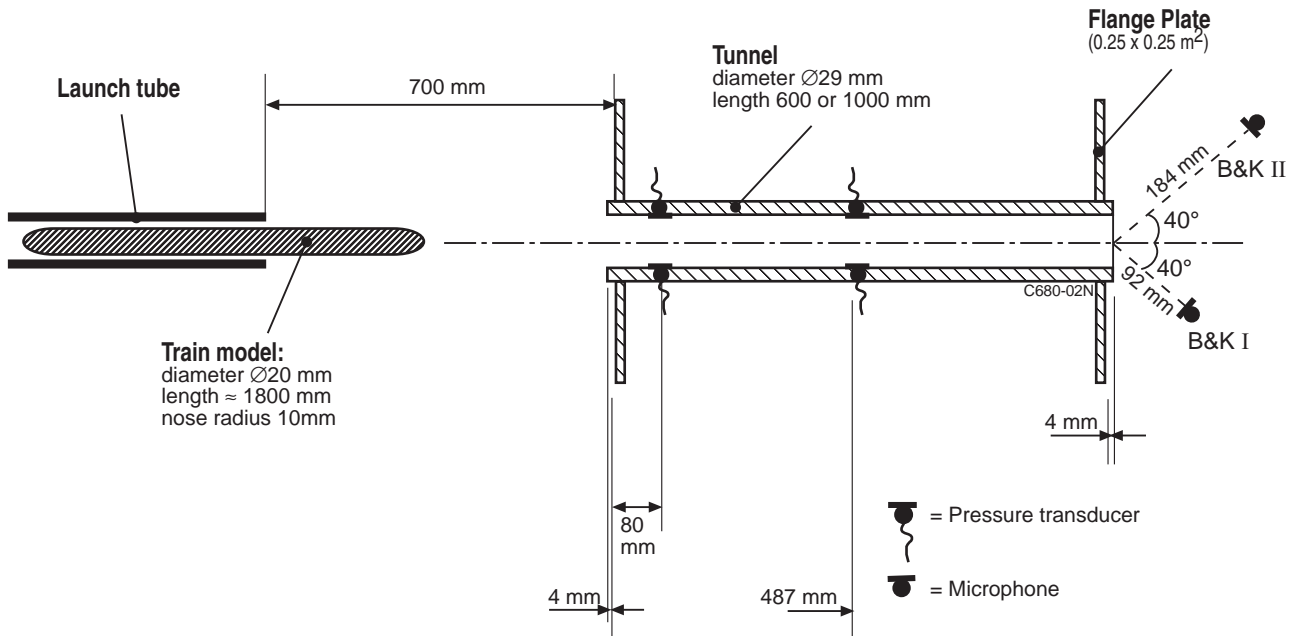


Fig. 8 Micro pressure wave test setup with short tunnel and high blockage ratio (48%)

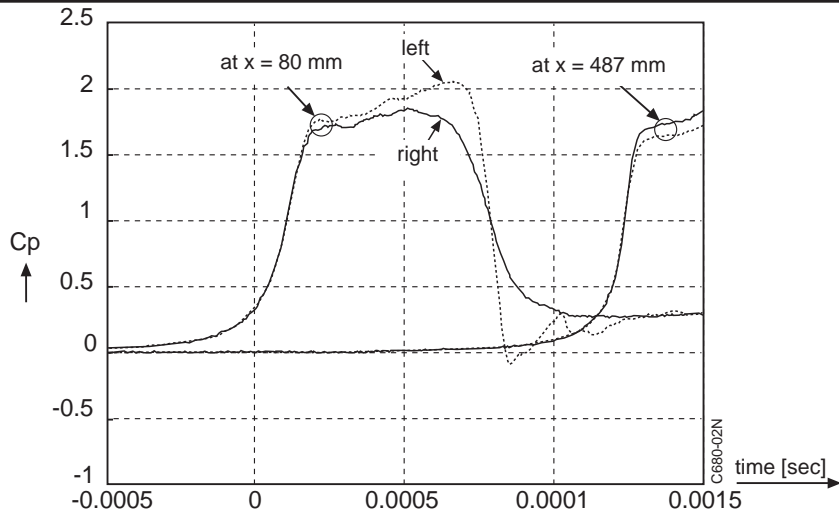


Fig. 9a Dimensionless pressure traces measured in the 1.0 m tunnel (Mt 6_10, train speed 91.0 m/s)

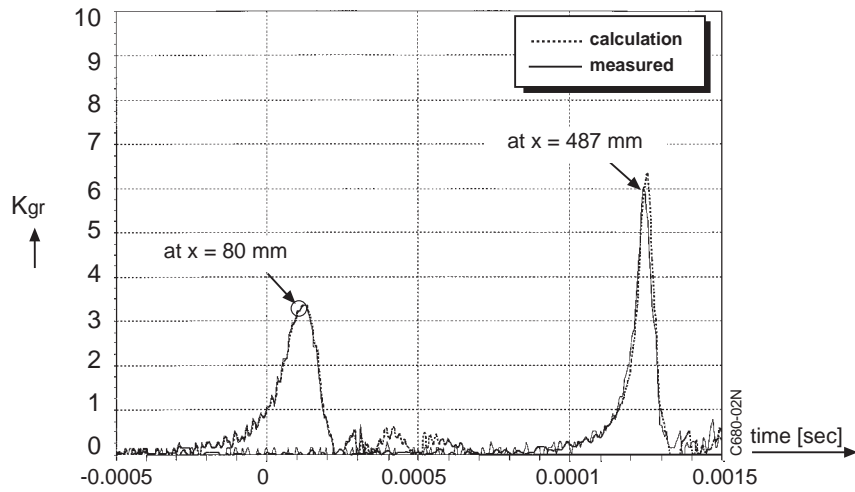


Fig. 9b Dimensionless pressure gradients (Mt 6_10)

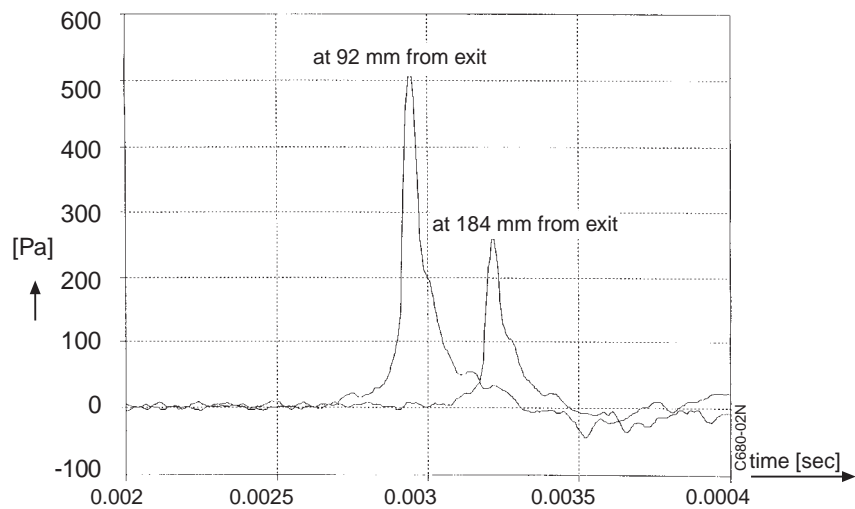


Fig. 9c Micro pressure wave recorded at 92 and 184 mm from the exit of the tunnel (Mt 6_10)

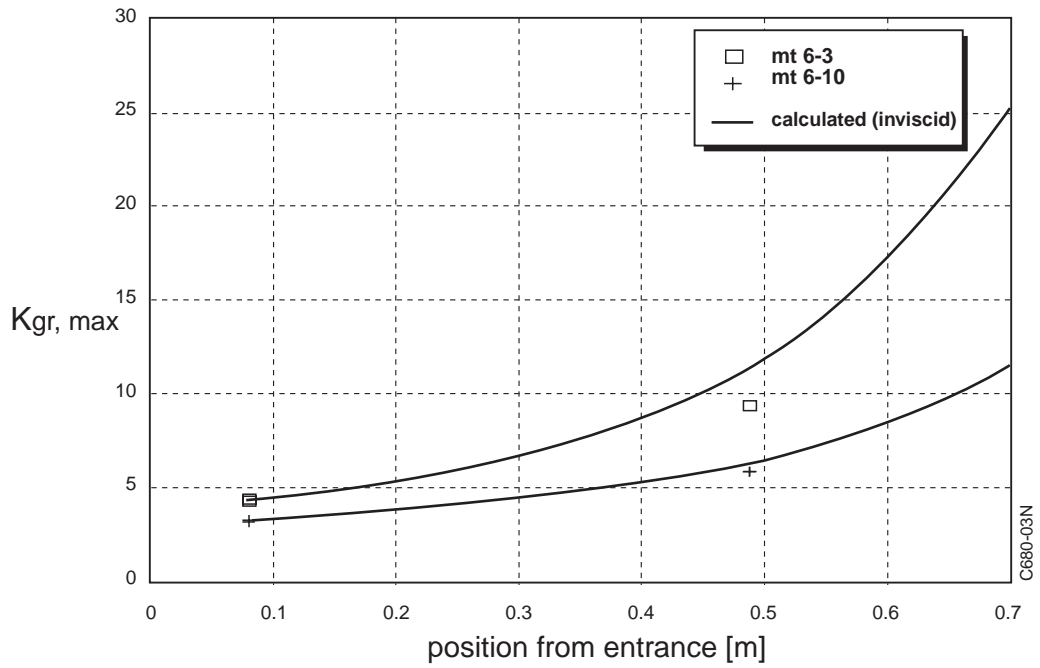


Fig. 10 Effect of the initial condition on the steeping of the pressure wave

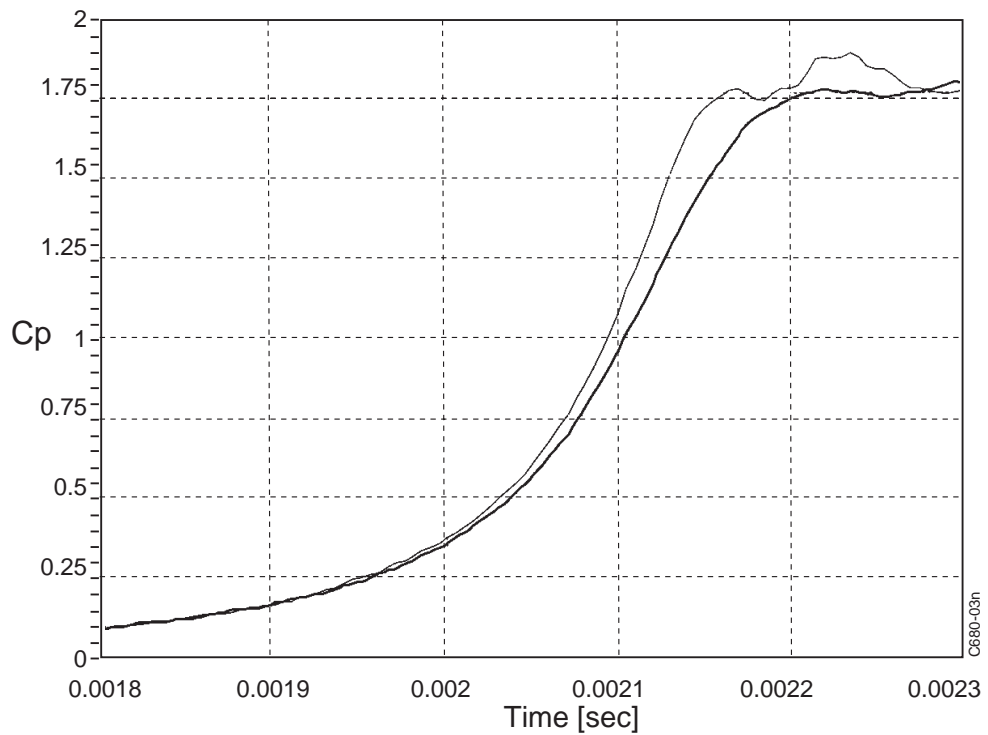


Fig. 11 Pressure traces of 6-3 and 6-10 at 80 mm from the entrance